Experimental Neurology 354 (2022) 114112

Contents lists available at ScienceDirect

Experimental Neurology

journal homepage: www.elsevier.com/locate/yexnr

Research paper

Close association of polarization and LC3, a marker of autophagy, in axon determination in mouse hippocampal neurons

Naoki Segi [a,b], Tomoya Ozaki [a], Yuji Suzuki [a], Jun Ouchida [a,b], Shiro Imagama [b], Kenji Kadomatsu [a,c,*], Kazuma Sakamoto [a,c,*]

[a] Department of Biochemistry, Nagoya University Graduate School of Medicine, 65 Tsurumai-cho, Showa-ku, Nagoya 466-8550, Japan
[b] Department of Orthopedics, Nagoya University Graduate School of Medicine, 65 Tsurumai-cho, Showa-ku, Nagoya 466-8550, Japan
[c] Institute for Glyco-core Research (iGCORE), Nagoya University, Furo-cho, Chikusa-ku, Nagoya 464-8601, Japan

ARTICLE INFO

Keywords:
Axon determination
Autophagy
Trehalose

ABSTRACT

The autophagy-lysosome pathway is a cellular clearance system for intracellular organelles, macromolecules and microorganisms. It is indispensable for cells not only to maintain their homeostasis but also to achieve more active cellular processes such as differentiation. Therefore, impairment or disruption of the autophagy-lysosome pathway leads to a wide spectrum of human diseases, ranging from several types of neurodegenerative diseases to malignancies. In elongating axons, autophagy preferentially occurs at growth cones, and disruption of autophagy is closely associated with incapacity for axonal regeneration after injury in the central nervous system. However, the roles of autophagy in developing neurons remain elusive. In particular, whether autophagy is involved in axon–dendrite determination is largely unclear. Using primary cultured mouse embryonic hippocampal neurons, we here showed the polarized distribution of autophagosomes among minor processes of neurons at stage 2. Time-lapse observation of neurons from GFP-LC3 transgenic mice demonstrated that an "LC3 surge"—*i.e.*, a rapid accumulation of autophagic marker LC3 that continues for several hours in one minor process—proceeded the differentiation of neurons into axons. In addition, pharmacological activation and inhibition of autophagy by trehalose and bafilomycin, respectively, accelerated and delayed axonal determination. Taken together, our findings revealed the close association between LC3, a marker of autophagy, and axon determination in developing neurons.

1. Introduction

Autophagy is an evolutionally conserved cellular machinery for the clearing away of cellular components in order to protect cells from damage by these unfavorable materials (Mizushima and Komatsu, 2011). It is also important for nutrition supply and is activated under starvation. Autophagy starts at the phagophore assembly site, where nucleated proteins and lipids form cup-like structures called phagophores or isolation membranes. As the membrane elongates, the isolation membrane closes to form an autophagosome that engulfs cytosolic materials including proteins, organelles, or microorganisms. Thereafter, the autophagosome fuses to a lysosome and releases its components into the lysosomal lumen to be degraded by lysosomal catabolic enzymes (Mizushima et al., 2011).

Many studies have demonstrated the clinical relevance of autophagy to human diseases (Mizushima and Levine, 2020). Several chemicals that can modulate cellular autophagic activity have been under clinical trials targeting neurodegenerative diseases, cancer and diabetes (Kroemer, 2015). In particular, autophagy is indispensable in the homeostasis of post-mitotic cells such as neurons. This is partially because these post-mitotic cells are not able to dilute toxic cytosolic materials by cell division (Nixon et al., 2008). Indeed, a conditional knockout mouse for *Atg7* in the neuronal lineage of the central nervous systems, whose protein product is essential for the formation of an autophagosomal membrane, displayed a neurodegenerative phenotype, and half of the animals died around five weeks after birth (Komatsu et al., 2006).

The mechanisms of autophagy in "polarized" or axon-elongating neurons are well documented. The autophagic machinery proteins such as ATG9 and ATG13 were specifically enriched at the distal end of axons or a growth cone. The isolation membranes are formed in close

Abbreviations: LC3, microtubule-associated protein light chain 3; GFP, green fluorescent protein.

* Corresponding author at: Department of Biochemistry, Nagoya University Graduate School of Medicine, 65 Tsurumai-cho, Showa-ku, Nagoya 466-8550, Japan.
E-mail addresses: kkadoma@med.nagoya-u.ac.jp (K. Kadomatsu), sakamoto@med.nagoya-u.ac.jp (K. Sakamoto).

https://doi.org/10.1016/j.expneurol.2022.114112
Received 26 January 2022; Received in revised form 28 April 2022; Accepted 6 May 2022
Available online 11 May 2022

proximity to the endoplasmic reticulum, and the autophagosomes are retrogradely transported toward soma, fusing with lysosomes (Maday et al., 2012; Maday and Holzbaur, 2014). Such spatially regulated autophagy in elongating neurons is thought to be important for the maintenance of axonal homeostasis with a high molecular turnover (Nixon, 2013). Indeed, our recent study demonstrated that the disruption of autophagy was closely associated with the inability of axons to regenerate after injury (Sakamoto et al., 2019; Sakamoto et al., 2021a; Sakamoto et al., 2021b). Scar-associated chondroitin sulfate activates neuronal receptor PTPσ (receptor-type protein tyrosine phosphatase sigma), leading to the tyrosine-dephosphorylation of cortactin, which in turn inhibits fusion between lysosome and autophagosome. As a result, the autophagosomes are abnormally accumulated in the distal terminal of the severed axons, transforming the terminal into a so-called "dystrophic endball," as first described by Cajal.

In contrast, little is known about the mechanism or significance of autophagy in unpolarized neurons. Mature neurons have a highly developed polarity, typically with a single axon and multiple dendrites, to process information through signal input, integration, and output to form neural networks. Based on the observation of spontaneous polarity formation using dispersed culture neurons derived from the rat hippocampus, the neuronal polarization process has been classified into five stages. At the start of culture, neurons first form lamellipodia (stage 1: several hours after plating). After that, a few immature neurites, called minor processes, grow out from the cell body (stage 2: 0.5 to 1.5 days). At this moment, the neurons are still symmetrical, and each minor process undergoes growth and retraction. One of these immature neurites elongates rapidly, breaking the symmetry to form the axon (stage 3: 1.5 to 3 days). The other minor processes develop into dendrites (stage 4: 4 to 7 days). Finally, the interneuronal connections are formed and synaptic transmissions are established (stage 5: >7 days) (Dotti et al., 1988; Arimura and Kaibuchi, 2007; Banker, 2018).

The extrinsic and intrinsic molecular machineries required to convert one minor process into an axon to determine one minor process as an axon have been extensively studied (Kishi et al., 2005; Yoshimura et al., 2005; Shelly et al., 2007; Zhang et al., 2007; Yi et al., 2010; Chen et al., 2013). However, as mentioned above, whether autophagy is involved in the axon specification has not been addressed. Here, based on live imaging of hippocampal neurons, we found that a spatially activated autophagy in a minor process accelerated axon specification at stage 2 to stage 3. Consistent with this finding the pharmaceutical modulation of autophagy in stage 2 neurons also affected axon polarization. Together, our data demonstrated that autophagy was closely associated with axon specification in developing neurons.

2. Materials and methods

2.1. Animals

C57BL/6 J mice were purchased from SLC Inc. (Japan). GFP-LC3 transgenic mice carrying a rat LC3 fused with GFP at the N-terminal under the control of the chick β-actin promoter were obtained from RIKEN BioResource Center (Kuma et al., 2004). Mice were housed in a temperature-controlled cage under a 12-h light/dark cycle, and received food and water *ad libitum*.

2.2. Primary culture of hippocampal neurons

Primary culture of hippocampal neurons from embryonic day 17 or 18 (E17 or 18) was carried out as reported elsewhere with minor modifications (Kaech and Banker, 2006). Briefly, hippocampal neurons were dissected from embryos and kept in ice-cold HBSS (Hank's balanced salt solution). The meninges were carefully removed with fine forceps under a microscope. The tissues were minced and incubated with TrypLE (Gibco) for 5 min at 37 °C The tissues were precipitated by a brief centrifuge and triturated into single cells using a fire-polished Pasteur pipette. The dissociated cells were suspended in Neurobasal Plus medium supplemented with 2% of B-27 Plus, GlutaMAX (x 100, Gibco) and Antibiotic-Antimycotic (Gibco). The cells were seeded onto PDL (poly-D-lysine, M.W. 50–100 kDa, 100 μg/mL, Gibco, A3890401) and laminin (10 μg/mL; Thermo Scientific)-coated glass-bottom dishes (IWAKI, 3911–035) and cultured until analysis. All experiments were designed to minimize the number of animals used and their suffering and pain based on international guidelines. All animal experiments were approved by the Committee of Animal Care of the Nagoya University School of Medicine.

2.3. Immunostaining

Primary cultured hippocampal neurons were fixed with 4% paraformaldehyde (PFA) for 10 min at room temperature and permeabilized with methanol at −30 °C for 1 min. The cells were then rinsed three times with phosphate-buffered saline (PBS) and incubated in a blocking solution containing 5% (v/v) normal goat serum (Vector Laboratories) and 0.1% (v/v) Triton X-100 for 90 min at room temperature. For neuron-specific class III β-tubulin (Tuj1) staining, samples were bathed in 1:1000 mouse monoclonal anti-Tuj1 (Covance, 801,201) diluted in PBS containing 2.5% (v/v) normal goat serum overnight at 4 °C After three washes with PBS, the neurons were incubated with 1:250 Alexa Fluor 488-conjugated goat anti-mouse IgG (1:250; Molecular Probes, A11001) diluted in PBS containing 2.5% (v/v) goat serum for 2 h at room temperature. For double staining for Tuj1 and LC3, samples were incubated with mouse monoclonal anti-Tuj1 (1:1000; Covance, 801,201) and rabbit monoclonal anti-LC3B (1:500; Cell Signaling Technology, 3868) dissolved in PBS containing 2.5% (v/v) goat serum overnight at 4 °C. After washing, these samples were incubated with secondary antibodies with Alexa Fluor488-conjugated goat anti-mouse IgG (1:250; Molecular Probes, A11001) and 1:250 Alexa Fluor 594-conjugated goat anti-rabbit IgG (1:250; Molecular Probes, A11012) diluted in PBS containing 2.5% (v/v) goat serum for 2 h at room temperature. For double staining for Tau and LC3, mouse monoclonal anti-Tau-1 (1:1000; Chemicon, MAB3420) and rabbit monoclonal anti-LC3B (1:500; Cell Signaling Technology, 3868) were used, and for double staining for Tuj1 and Tau, rabbit polyclonal anti-Tuj1 (1:1000; Covance, 802,001) and mouse monoclonal anti-Tau-1 (1:1000; Chemicon, MAB3420) were used, respectively. The samples were then thoroughly washed with PBS and embedded with FluorSave mounting medium (Millipore).

2.4. Image acquisition

Fluorescent images were obtained using a TiEA1R microscope (Nikon) equipped with a Plan Apo VC 60 × A WI DIC N2 water immersion objective lens (N.A. = 1.2, Nikon) and a GaAsP detector (Nikon) in a fixed image acquisition setting. Digital images were processed and analyzed using ImageJ. NeuronJ (Meijering et al., 2004) was used to recognize all neurites using Tuj1-stained images, and then MeasureROIs plug-ins were used to convert them into ImageJ compliant ROIs to measure the length of neurites. The soma was excluded from the analysis.

2.5. Live-cell imaging

Neurons were time-lapse imaged in a recording chamber where CO_2 concentration (5%), temperature (37 °C, and humidity were maintained. For long time-lapse imaging to capture the transition of neurons from stage 2 to stage 3, the images were acquired with a TiEA1R microscope (Nikon) with a Plan Apo 40× DIC M N2 objective lens (N. A. = 0.95, Nikon), a Perfect Focus System (Nikon), and a GaAsP detector (Nikon). 512 × 512-pixel images were taken continuously every 5 min. Digital images were processed and analyzed using ImageJ. As with immunostaining, NeuronJ and MeasureROIs plug-ins were used to acquire

neurite ROIs in differential interference contrast images, from which neurite length and GFP-LC3 intensity were measured. The number of GFP-LC3 puncta inside the ROI were counted visually for each neurite; two examiners (N.S. and T.O.) counted each puncta individually, and the smaller number was adopted.

2.6. Statistics and reproducibility

No statistical methods were used to determine the sample size of the experiment. Unless otherwise noted, data are presented as mean values with standard deviation. The data sets were analyzed using unpaired *t*-test to compare between two groups; in cases of three or more groups, a one-way analysis of variance (ANOVA) was applied in combination with a *post hoc* Tukey test to correct for multiple comparisons. Pearson's correlation coefficient was used to examine the correlation. Statistical analyses were performed using R version 4.1.0 (http://www.R-project.org). Values of $p < 0.05$ were considered statistically significant. Each experiment was independently repeated at least three times. All samples or animals were included in the analysis. Experiments were not randomized and were conducted in an unblinded fashion.

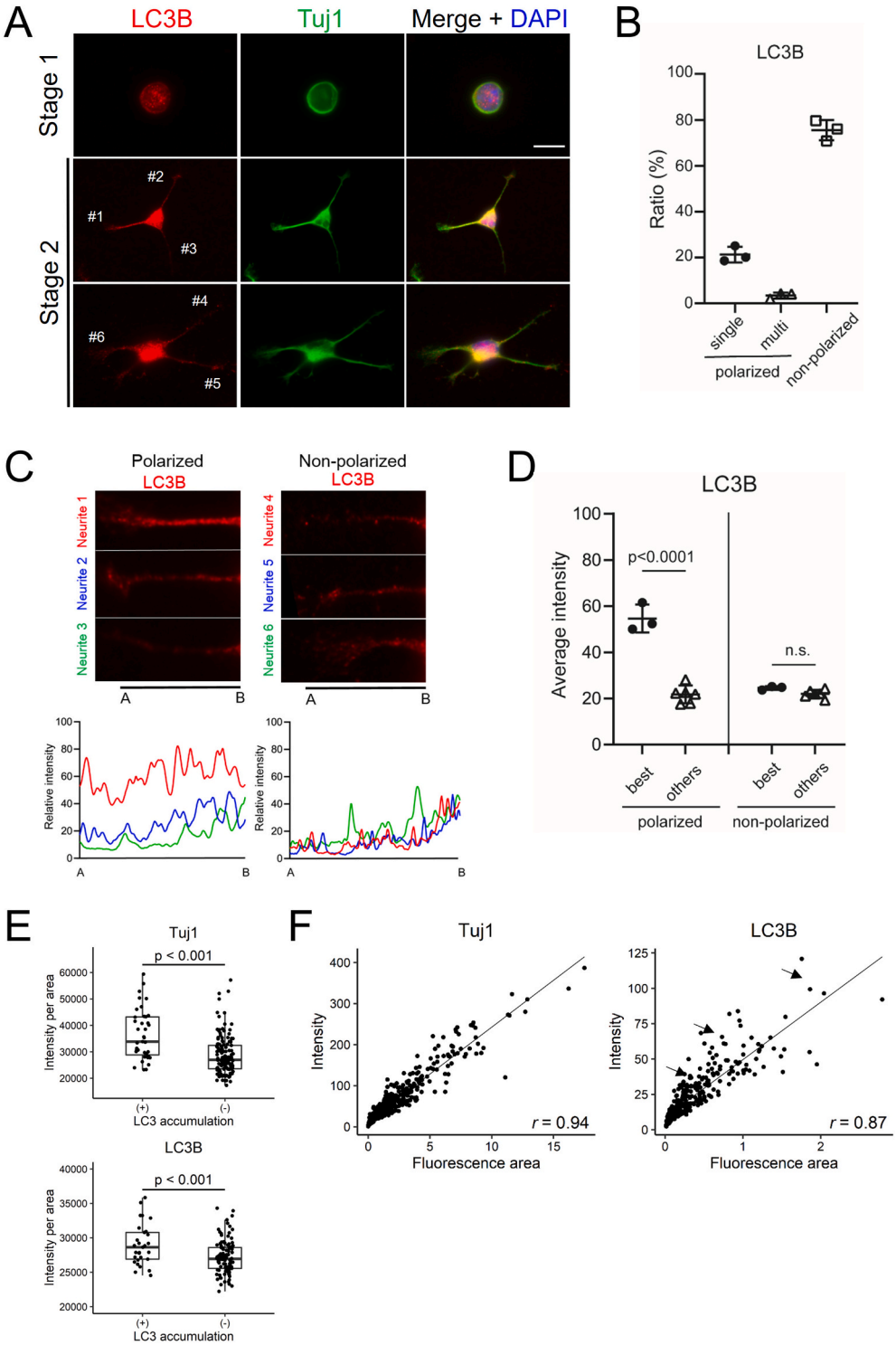

Fig. 1. Polarized localization of autophagosomes in minor processes at stage 2.
A. Immunocytochemistry for LC3B and Tuj1 of hippocampal neurons at stage 1 and stage 2. Scale bar, 10 μm. B. The ratio of polarized neurons at stage 2. The results are presented as means ± S.D. (n = 3 dishes, total 152 neurons). C. The higher magnification of six minor processes of the stage 2 neurons at the bottom panel of (A). The line plot analysis for LC3B is also shown. D. The average intensity of LC3B in the best polarized neurite and the rest neurites (n = 3 neurons, unpaired *t*-test). E. Fluorescence intensity per detected area of Tuj1 (top) and LC3B (bottom) in minor processes with or without LC3 accumulation (n = 491 minor processes, unpaired *t*-test). F. Correlation between the fluorescence detection area and fluorescence intensity for Tuj1 (left) and LC3B (right) in minor processes. There was a stronger correlation for Tuj1 (Pearson's correlation coefficient, r = 0.94) than for LC3B (r = 0.87); arrows show the outliers of fluorescence intensity to fluorescence detection area (n = 491 minor processes).

3. Results

3.1. Polarized distribution of autophagosomes in neurons at stage 2

To investigate whether autophagy was involved in determination of the dendro–axonal fate, we carried out immunocytochemistry for LC3B, a marker for autophagosomes in primary cultured immature primary neurons (Kabeya et al., 2000). At stage 1, autophagosomes were located equally throughout the cytosol (Fig. 1A). At stage 2, we observed two types of neurons with respect to the localization of autophagosomes, *i.e.*, polarized (Fig. 1A, middle panel) and non-polarized (Fig. 1A, bottom panel). In the polarized neurons, autophagosomes seemed to be enriched in one minor process rather than multiple processes (Fig. 1B to Fig. 1D). This population accounted for approximately 20% of the neurons at stage 2 (Fig. 1B). In contrast, the majority of neurons at stage 2 showed non-polarized distribution of autophagosomes, in which similar numbers of autophagosomes were located among minor processes (Fig. 1B to Fig. 1D).

The class III β-tubulin (Tuj1) signals also showed the polarized pattern in some neurons (Fig. 1A), which might have been due to the difference in the length and the diameter of each minor process. To exclude potential bias, we compared the relationship between the fluorescence detection area and integrated fluorescence intensity for Tuj1 and LC3B for all minor processes in neurons at stage 2. Although both Tuj1 and LC3B showed a significant increase in fluorescence intensity in the LC3B-accumulated minor processes (Fig. 1E), further scatter plot analysis revealed that Tuj1 had a stronger linear relationship between intensity and area (Pearson's correlation coefficient, r = 0.94, n = 491 neurites), indicating that Tuj1 was equally distributed to all minor processes at stage 2 (Fig. 1F, left). In contrast, LC3B showed a relatively

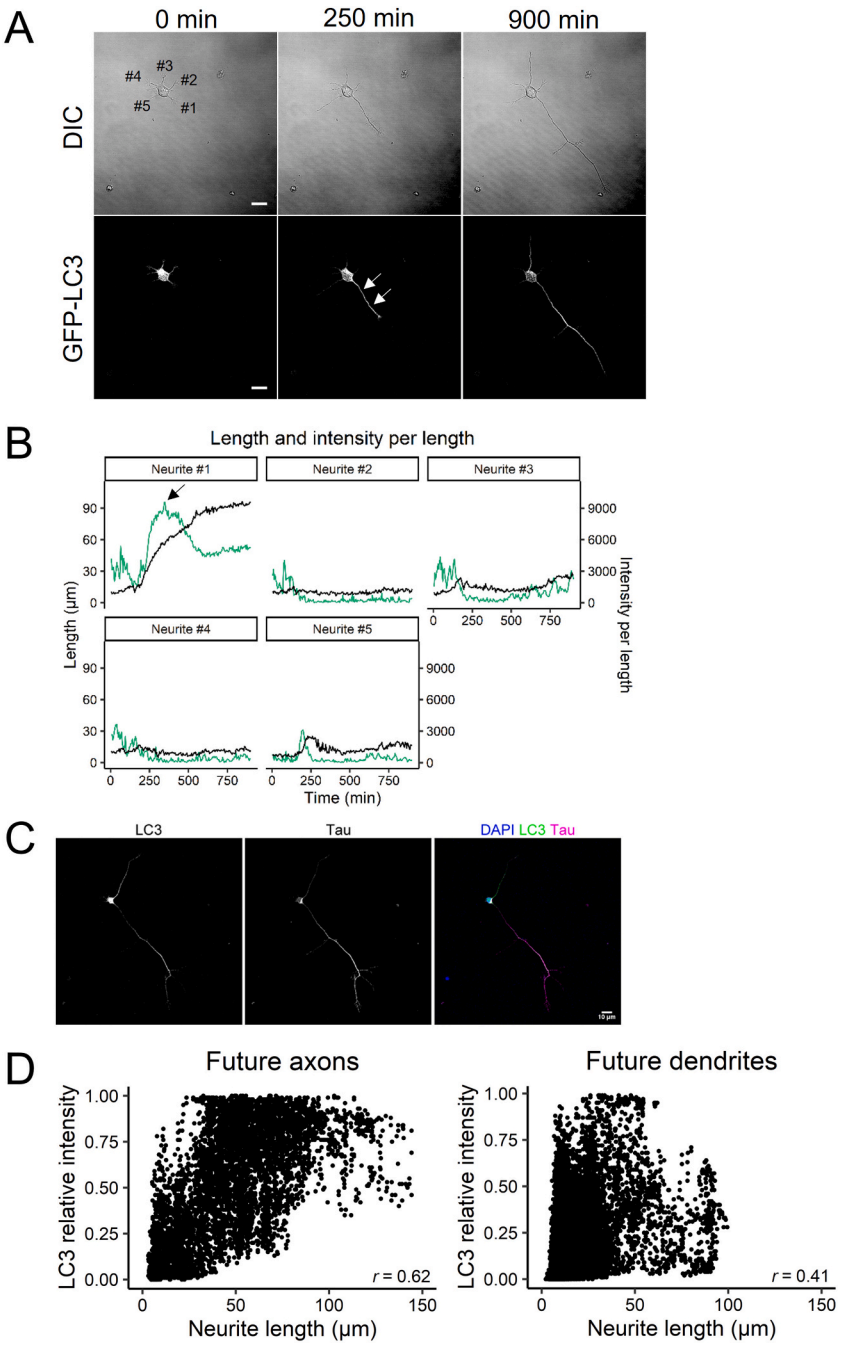

Fig. 2. LC3 surge drove axonal specification.
A. Time-lapse recording of hippocampal neurons from GFP-LC3 transgenic mice at stages 2 to 3. The images were obtained with a 40× object lens every 5 min. The arrow indicates polarized accumulation of autophagosomes in neurite #1 followed by its axonal specification. Scale bar, 10 μm. B. The length (black) and the relative intensity of GFP-LC3 (green) in five minor processes in (A). The relative intensity was calculated based on the average value of the intensities of all minor processes. Note that the axonal specification of neurite #1 occurred just after the "LC3 surge" (arrow). See also Video 1. C. Immunocytochemistry for Tau confirmed that neurite #1 in (A) was specified into an axon. Scale bar, 10 μm. D. The retrospective analysis of axon and dendrite for their length and relative intensity of LC3 before axon determination (n = 23 neurons, at 5903 time points). A positive correlation between length and intensity was observed in future axon (r = 0.62) with higher correlation coefficient compared with future dendrite (r = 0.41). (For interpretation of the references to colour in this figure legend, the reader is referred to the web version of this article.)

low correlation (r = 0.87), with a disproportionately high intensity for area (Fig. 1F, right, arrows), suggesting that LC3B was indeed accumulated in some minor processes. Because one minor process should be selected as an axon at stage 2 to stage 3, the results above led us to study whether autophagy was a determinant for the axonal fate in developing neurons.

3.2. "LC3 surge" drove a minor process to an axon

To further address the relationship between autophagy and axon determination, we conducted a time-lapse imaging of primary cultured hippocampal neurons obtained from GFP-LC3 transgenic mice at stages 2 to 3. Twelve hours after seeding, the neurons at stage 2 were picked up and began to be observed under a confocal microscope. We observed the oscillated distribution of autophagosomes among the minor processes. However, at one point, there was a rapid augmentation of GFP signals (LC3 surge, hereafter) in one minor process that persisted for several hours (Fig. 2A). Along with the LC3 surge, the minor process started to elongate and the neuron obtained polarity (Fig. 2B, arrow and Video 1). After the live imaging, the same neurons were fixed and stained with axonal marker Tau to confirm that the neurite which was elongated after the LC3 surge differentiated into an axon (Kosik and Finch, 1987) (Fig. 2C). The retrospective analysis for the relative and maximum intensity for GFP-LC3 in minor processes in stage 2 neurons also showed that the future axons had significantly higher autophagic activity than the future dendrites (Fig. 2D).

3.3. Forced activation of autophagy in developing neurons facilitated axonal determination

Trehalose is a disaccharide from natural sources and has been shown to activate autophagy in an mTOR-independent manner (Sarkar et al., 2007). To investigate whether or not activated autophagy affects neuronal polarization, we treated hippocampal neurons at stage 2 with 25 mM of trehalose (Fig. 3A). As expected, trehalose promptly induced autophagy in minor processes and the effect lasted for more than 200 min, as examined by the intensity of GFP-LC3 and GFP-positive puncta (Fig. 3B and Fig. 3C). The buff treatment of trehalose induced autophagy in multiple or all neurites rather than a single neurite (Fig. 3D).

The morphology of the neurons was assessed by calculating the ratio of the length of the longest neurite to that of the second longest neurite. As shown in Fig. 4A, trehalose significantly enhanced the elongation of

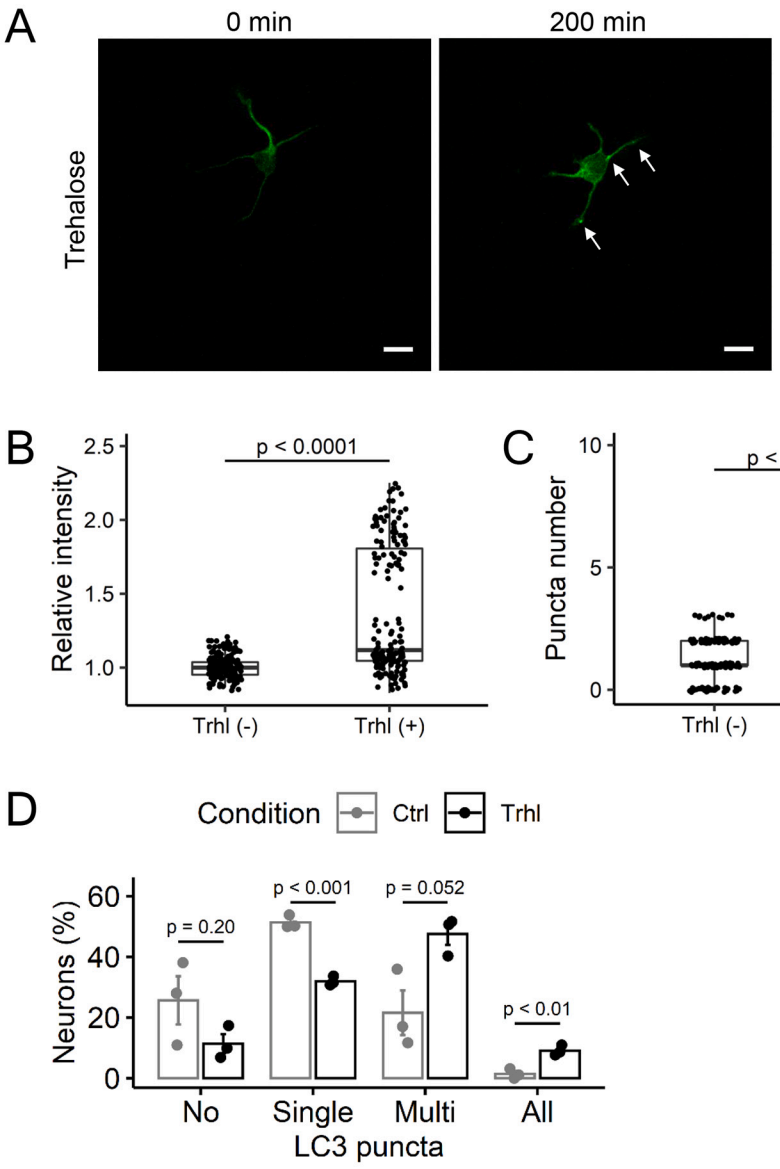

Fig. 3. Trehalose induced autophagy in neurons.
A. Trehalose (25 mM final concentration) was added to the medium of stage 2 hippocampal neurons. The arrows indicate GFP-LC3-positive puncta. Scale bar, 10 μm. B. The relative intensity for GFP-LC3 in minor processes before and after trehalose supplementation. The relative intensity was calculated based on the average value of the intensities of all minor processes (n = 163 neurites, unpaired *t*-test). C. The number of GFP-LC3-positive puncta (autophagosomes) before and after trehalose supplementation (n = 163 neurites, unpaired *t*-test). D. The ratio of neurons classified by the number of neurites with accumulation of LC3 puncta induced by trehalose (n = 3 dishes each, unpaired *t*-test).

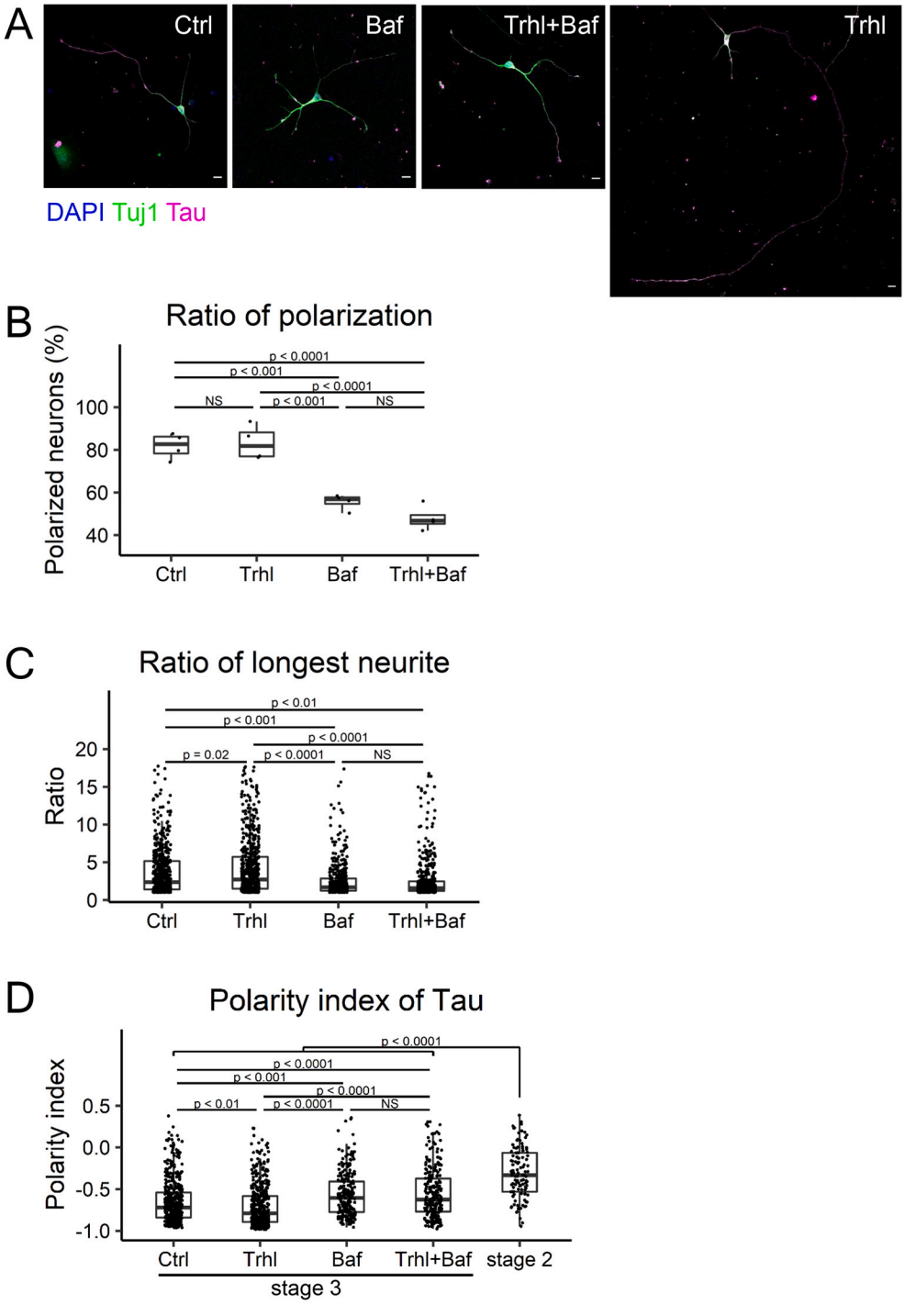

Fig. 4. Trehalose accelerated axon specification in hippocampal neurons.
A. Immunocytochemistry for Tau (magenta) and Tuj1 (green) for hippocampal neurons. Neurons were treated the indicated drugs (25 mM trehalose or 10 μM bafilomycin A1) six hours later after seeding for 2 days. Scale bar, 10 μm. B. The ratio of neurons after the treatment of indicated drugs for 2 days (n = 4 dishes each, one-way ANOVA with post-hoc Tukey HSD). C. The ratio of the length of an axon to a dendrite (n = 308 for "Ctrl", 311 for "Trhl", 265 for "Baf", and 269 neurons for "Trhl+Baf", one-way ANOVA with post-hoc Tukey test). D. The polarity index (PI) was calculated based on Tau signals. PI>0 or PI<0 indicates polarization toward dendrites or axons, respectively. (n = 308 for "Ctrl", 311 for "Trhl", 265 for "Baf", 269 for "Trhl+Baf" and n = 111 for "stage 2" neurons, one-way ANOVA with post-hoc Tukey test). (For interpretation of the references to colour in this figure legend, the reader is referred to the web version of this article.)

the longest neurite. Consistent with this finding, the treatment of neurons with bafilomycin A1 (Baf), a vacuolar H^+-ATPase inhibitor, which disrupts autophagy flux by inhibiting lysosomal fusion to autophagosomes, in turn suppressed the outgrowth of the longest neurite (Fig. 4A and Fig. 4B). Bafilomycin A1 also canceled trehalose-induced elongation of the neurite (Fig. 4A to Fig. 4C).

To further assess the biological properties of the neurites, we calculated the polarity index (PI) (Kapitein and Hoogenraad, 2015) of Tau. PI was calculated as PI = (Id - Ia) / (Id + Ia), where Id is the average intensity of Tau in dendrites and Ia is the intensity of Tau of the axon. PI>0 or PI<0 is a value indicating polarization toward dendrites or axons, respectively. As shown in Fig. 4D, trehalose significantly decreased PI, while bafilomycin A1 significantly increased PI. Again, the effect of trehalose was counteracted by bafilomycin A1.

4. Discussion

In our past study, we demonstrated the role of autophagy after axonal injury. Chondroitin sulfate, one of the major inhibitory cues for axonal regeneration after injury in the CNS (Bradbury et al., 2002; Silver and Miller, 2004; Kadomatsu and Sakamoto, 2014; Sakamoto and Kadomatsu, 2017), activates neuronal receptor PTPσ (Shen et al., 2009; Coles et al., 2011), which induces the tyrosine dephosphorylation of cortactin, resulting in an attenuation of the fusion between

autophagosomes and lysosomes (Sakamoto et al., 2019; Sakamoto et al., 2021b). That leads to abnormal accumulation of autophagosomes at the distal tip of the severed axons, transforming them into so-called endballs with poor regenerative activity. These findings prompted us to investigate the putative roles of autophagy in more immature neurons, especially during axonal polarization.

We utilized the well-established model of primary cultured hippocampal neurons to investigate this issue (Dotti et al., 1988). As expected, but intriguingly nonetheless, only a subpopulation of neurons showed the polarized distribution of autophagosomes among minor processes at stage 2 (Fig. 1A to Fig. 1D). Because stage 2 lasts approximately one day (Dotti et al., 1988), it might be considered that not all neurons exhibited the polarity. Based on live imaging of stage 2 neurons from GFP-LC3 transgenic mice, we found a sudden activation of autophagy in only one neurite that lasted several hours (Fig. 2). Subsequently, the neurite suddenly began to elongate into an axon (Fig. 2). These results suggested that asymmetric activation of autophagy in minor processes is involved in axon determination.

To activate autophagy in the minor processes of hippocampal neurons at stage 2, we used trehalose, which can induce autophagy by unknown mechanisms. We expected that trehalose would induce multipolar neurons with multiple axons, as reported with other positive cues (Da Silva et al., 2005; Kishi et al., 2005; Yoshimura et al., 2005; Barnes et al., 2007) because it induced LC3 accumulation in all minor processes (Fig. 3D). Unexpectedly, however, trehalose simply accelerated the axon specifications of one neurite (Fig. 4A to Fig. 4C). Although we cannot provide any reasonable explanation for this finding, it is intriguing if we consider that the depletion of Atg5 delayed the maturation of adult newborn neurons (Xi et al., 2016).

How autophagy specified one neurite into an axon was not clarified in the current study. One possible explanation is that autophagy regulates local positive signals for axon specification. For example, Trk family proteins are localized at the tip of a minor process, and their activation by neurotrophins such as NT-3 and brain-derived neurotrophic factor (BDNF) promotes axon determination through the Ras and PI3K-AKT pathways (Segal, 2003; Yoshimura et al., 2005; Kim et al., 2006; Arimura and Kaibuchi, 2007). The endocytosed Trk is retrogradely transported toward the soma on microtubes. This retrograde transport of Trk has been shown to be important for its full activity (Segal, 2003; Glebova and Ginty, 2005). It was also revealed that BDNF-activated TrkB was endocytosed and translocated to the autophagosome in AP-2-dependent manner in neurons, and that this translocation was important for neurons to acquire their complexity *in vivo* (Kononenko et al., 2017). Therefore, it is possible that the local autophagy and its retrograde transport are involved in the regulation of Trk signaling at the time of the axon–dendrite fate decision.

The role of autophagy in the central nervous systems (CNS) has attracted much attention. In particular, much effort has been paid to the significance of autophagy in terminally differentiated mature neurons. Indeed, its impairment has been shown to be closely associated with neurodegenerative disease. For example, the insertion or deletion of *WDR45,* which encodes WIPI14, an essential protein for biogenesis of the isolation membrane, causes SENDA (static encephalopathy of childhood with neurodegeneration in adulthood) (Saitsu et al., 2013). Accumulating evidence indicates that disruption of mitophagy leads to Parkinson's disease (PD), in which reactive oxygen species (ROS) from damaged mitochondria damage neurons (Kitada et al., 1998; Valente et al., 2004; Okatsu et al., 2015; Wauer et al., 2015; Akabane et al., 2016). The impairment of trafficking of autophagosomes also causes neurodegeneration. For example, a dysfunction of dynactin, an activator for dynein which is essential for the retrograde transport of autophagosomes on microtubules, is associated with two different types of neurodegenerative diseases, Perry syndrome and lower motor neuron disease (Puls et al., 2003; Farrer et al., 2009). Spinal-bulbar muscular atrophy (SBMA) is an X-linked recessive inheritance disease with a progressive loss of neurons in the brainstem and spinal cord. It is caused by the insertion and elongation of the CAG repeat in the first exon of androgen receptor (AR) genes, which produces poly-glutamine AR (polyQ-AR) (La Spada et al., 1991). The wild-type AR can interact with and activate transcription factor EB (TFEB), which both participates in and serves as a master regulator for the CLEAR (coordinated lysosomal enhancement and regulation) network (Settembre et al., 2013), and maintain the homeostasis of the autophagosome–lysosome pathway. In contrast, polyQ-AR, which can still interact with TFEB, inhibits the activity of TFEB.

Collectively, our results demonstrated the close association of autophagic marker LC3 and axonal determination. Further analysis is warranted, particularly in regard to the *in vivo* significance of autophagy and its disruption in neurodevelopmental disorders such as autism.

5. Conclusions

Autophagy has attracted much attention for its relevance to neurodegenerative diseases. However, the biological significance of autophagy in the acquisition of morphological polarity by neurons has not been elucidated. Here, based on live-imaging of primary cultured hippocampal neurons from GFP-LC3 transgenic mice, we observed a polarized activation of autophagy that lasted for several hours in a single minor process at stage 2. This LC3 surge led to the rapid elongation of the minor process, which finally resulted in its differentiation into the axon. Consistent with these findings the pharmacological activation of autophagy by trehalose accelerated axon specification. Taken together, our results demonstrate the close association between autophagic marker LC3 and axon specification in neurons.

Supplementary data to this article can be found online at https://doi.org/10.1016/j.expneurol.2022.114112.

Author contributions

N.S. T.O. and K.S. designed the study and performed measurements. N.S., T.O., Y.S., J.O., S.I. and K.S. carried out the experiments. N.S., K.K and K.S. wrote the manuscript.

Declaration of Competing Interest

The authors declare no competing interests.

Acknowledgements

We thank Dr. Noboru Mizushima, Department of Biochemistry and Molecular Biology, Graduate School and Faculty of Medicine, The University of Tokyo, for providing us with GFP-LC3 transgenic mice.

This work was supported by JSPS KAKENHI Grant Numbers 19H03415 and 21K18251 to K.K. and 19K07348 to K.S, and TERUMO life science foundation to K.S. and DAIKO foundation to K.S.

References

Akabane, S., Uno, M., Tani, N., Shimazaki, S., Ebara, N., Kato, H., Kosako, H., Oka, T., 2016. PKA regulates PINK1 stability and Parkin recruitment to damaged mitochondria through phosphorylation of MIC60. Mol. Cell 62, 371–384.

Arimura, N., Kaibuchi, K., 2007. Neuronal polarity: from extracellular signals to intracellular mechanisms. Nat. Rev. Neurosci. 8, 194–205.

Banker, G., 2018. The development of neuronal polarity: a retrospective view. J. Neurosci. 38, 1867–1873.

Barnes, A.P., Lilley, B.N., Pan, Y.A., Plummer, L.J., Powell, A.W., Raines, A.N., Sanes, J. R., Polleux, F., 2007. LKB1 and SAD kinases define a pathway required for the polarization of cortical neurons. Cell 129, 549–563.

Bradbury, E.J., Moon, L.D., Popat, R.J., King, V.R., Bennett, G.S., Patel, P.N., Fawcett, J. W., McMahon, S.B., 2002. Chondroitinase ABC promotes functional recovery after spinal cord injury. Nature 416, 636–640.

Chen, S., Chen, J., Shi, H., Wei, M., Castaneda-Castellanos, D.R., Bultje, R.S., Pei, X., Kriegstein, A.R., Zhang, M., Shi, S.H., 2013. Regulation of microtubule stability and organization by mammalian Par3 in specifying neuronal polarity. Dev. Cell 24, 26–40.

Coles, C.H., Shen, Y., Tenney, A.P., Siebold, C., Sutton, G.C., Lu, W., Gallagher, J.T., Jones, E.Y., Flanagan, J.G., Aricescu, A.R., 2011. Proteoglycan-specific molecular switch for RPTPσ clustering and neuronal extension. Science 332, 484–488.
Da Silva, J.S., Hasegawa, T., Miyagi, T., Dotti, C.G., Abad-Rodriguez, J., 2005. Asymmetric membrane ganglioside sialidase activity specifies axonal fate. Nat. Neurosci. 8, 606–615.
Dotti, C.G., Sullivan, C.A., Banker, G.A., 1988. The establishment of polarity by hippocampal neurons in culture. J. Neurosci. 8, 1454–1468.
Farrer, M.J., et al., 2009. DCTN1 mutations in Perry syndrome. Nat. Genet. 41, 163–165.
Glebova, N.O., Ginty, D.D., 2005. Growth and survival signals controlling sympathetic nervous system development. Annu. Rev. Neurosci. 28, 191–222.
Kabeya, Y., Mizushima, N., Ueno, T., Yamamoto, A., Kirisako, T., Noda, T., Kominami, E., Ohsumi, Y., Yoshimori, T., 2000. LC3, a mammalian homologue of yeast Apg8p, is localized in autophagosome membranes after processing. EMBO J. 19, 5720–5728.
Kadomatsu, K., Sakamoto, K., 2014. Mechanisms of axon regeneration and its inhibition: roles of sulfated glycans. Arch. Biochem. Biophys. 558, 36–41.
Kaech, S., Banker, G., 2006. Culturing hippocampal neurons. Nat. Protoc. 1, 2406–2415.
Kapitein, L.C., Hoogenraad, C.C., 2015. Building the neuronal microtubule cytoskeleton. Neuron 87, 492–506.
Kim, W.Y., Zhou, F.Q., Zhou, J., Yokota, Y., Wang, Y.M., Yoshimura, T., Kaibuchi, K., Woodgett, J.R., Anton, E.S., Snider, W.D., 2006. Essential roles for GSK-3s and GSK-3-primed substrates in neurotrophin-induced and hippocampal axon growth. Neuron 52, 981–996.
Kishi, M., Pan, Y.A., Crump, J.G., Sanes, J.R., 2005. Mammalian SAD kinases are required for neuronal polarization. Science 307, 929–932.
Kitada, T., Asakawa, S., Hattori, N., Matsumine, H., Yamamura, Y., Minoshima, S., Yokochi, M., Mizuno, Y., Shimizu, N., 1998. Mutations in the parkin gene cause autosomal recessive juvenile parkinsonism. Nature 392, 605–608.
Komatsu, M., Waguri, S., Chiba, T., Murata, S., Iwata, J., Tanida, I., Ueno, T., Koike, M., Uchiyama, Y., Kominami, E., Tanaka, K., 2006. Loss of autophagy in the central nervous system causes neurodegeneration in mice. Nature 441, 880–884.
Kononenko, N.L., Claßen, G.A., Kuijpers, M., Puchkov, D., Maritzen, T., Tempes, A., Malik, A.R., Skalecka, A., Bera, S., Jaworski, J., Haucke, V., 2017. Retrograde transport of TrkB-containing autophagosomes via the adaptor AP-2 mediates neuronal complexity and prevents neurodegeneration. Nat. Commun. 8, 14819.
Kosik, K.S., Finch, E.A., 1987. MAP2 and tau segregate into dendritic and axonal domains after the elaboration of morphologically distinct neurites: an immunocytochemical study of cultured rat cerebrum. J. Neurosci. 7, 3142–3153.
Kroemer, G., 2015. Autophagy: a druggable process that is deregulated in aging and human disease. J. Clin. Invest. 125, 1–4.
Kuma, A., Hatano, M., Matsui, M., Yamamoto, A., Nakaya, H., Yoshimori, T., Ohsumi, Y., Tokuhisa, T., Mizushima, N., 2004. The role of autophagy during the early neonatal starvation period. Nature 432, 1032–1036.
La Spada, A.R., Wilson, E.M., Lubahn, D.B., Harding, A.E., Fischbeck, K.H., 1991. Androgen receptor gene mutations in X-linked spinal and bulbar muscular atrophy. Nature 352, 77–79.
Maday, S., Holzbaur, E.L., 2014. Autophagosome biogenesis in primary neurons follows an ordered and spatially regulated pathway. Dev. Cell 30, 71–85.
Maday, S., Wallace, K.E., Holzbaur, E.L., 2012. Autophagosomes initiate distally and mature during transport toward the cell soma in primary neurons. J. Cell Biol. 196, 407–417.
Meijering, E., Jacob, M., Sarria, J.C., Steiner, P., Hirling, H., Unser, M., 2004. Design and validation of a tool for neurite tracing and analysis in fluorescence microscopy images. Cytometry A 58, 167–176.
Mizushima, N., Komatsu, M., 2011. Autophagy: renovation of cells and tissues. Cell 147, 728–741.
Mizushima, N., Levine, B., 2020. Autophagy in human diseases. N. Engl. J. Med. 383, 1564–1576.
Mizushima, N., Yoshimori, T., Ohsumi, Y., 2011. The role of Atg proteins in autophagosome formation. Annu. Rev. Cell Dev. Biol. 27, 107–132.
Nixon, R.A., 2013. The role of autophagy in neurodegenerative disease. Nat. Med. 19, 983–997.
Nixon, R.A., Yang, D.S., Lee, J.H., 2008. Neurodegenerative lysosomal disorders: a continuum from development to late age. Autophagy 4, 590–599.
Okatsu, K., Koyano, F., Kimura, M., Kosako, H., Saeki, Y., Tanaka, K., Matsuda, N., 2015. Phosphorylated ubiquitin chain is the genuine Parkin receptor. J. Cell Biol. 209, 111–128.
Puls, I., Jonnakuty, C., LaMonte, B.H., Holzbaur, E.L., Tokito, M., Mann, E., Floeter, M.K., Bidus, K., Drayna, D., Oh, S.J., Brown, R.H., Ludlow, C.L., Fischbeck, K.H., 2003. Mutant dynactin in motor neuron disease. Nat. Genet. 33, 455–456.
Saitsu, H., et al., 2013. De novo mutations in the autophagy gene WDR45 cause static encephalopathy of childhood with neurodegeneration in adulthood. Nat. Genet. 45 (445–449), 449e441.
Sakamoto, K., Kadomatsu, K., 2017. Mechanisms of axon regeneration: the significance of proteoglycans. Biochim. Biophys. Acta Gen. Subj. 1861, 2435–2441.
Sakamoto, K., Ozaki, T., Ko, Y.C., Tsai, C.F., Gong, Y., Morozumi, M., Ishikawa, Y., Uchimura, K., Nadanaka, S., Kitagawa, H., Zulueta, M.M.L., Bandaru, A., Tamura, J. I., Hung, S.C., Kadomatsu, K., 2019. Glycan sulfation patterns define autophagy flux at axon tip via PTPRsigma-cortactin axis. Nat. Chem. Biol. 15, 699–709.
Sakamoto, K., Ozaki, T., Kadomatsu, K., 2021a. Axonal regeneration by glycosaminoglycan. Front. Cell Dev. Biol. 9, 702179.
Sakamoto, K., Ozaki, T., Suzuki, Y., Kadomatsu, K., 2021b. Type IIa RPTPs and glycans: roles in axon regeneration and synaptogenesis. Int. J. Mol. Sci. 22.
Sarkar, S., Davies, J.E., Huang, Z., Tunnacliffe, A., Rubinsztein, D.C., 2007. Trehalose, a novel mTOR-independent autophagy enhancer, accelerates the clearance of mutant huntingtin and alpha-synuclein. J. Biol. Chem. 282, 5641–5652.
Segal, R.A., 2003. Selectivity in neurotrophin signaling: theme and variations. Annu. Rev. Neurosci. 26, 299–330.
Settembre, C., Fraldi, A., Medina, D.L., Ballabio, A., 2013. Signals from the lysosome: a control centre for cellular clearance and energy metabolism. Nat. Rev. Mol. Cell Biol. 14, 283–296.
Shelly, M., Cancedda, L., Heilshorn, S., Sumbre, G., Poo, M.M., 2007. LKB1/STRAD promotes axon initiation during neuronal polarization. Cell 129, 565–577.
Shen, Y., Tenney, A.P., Busch, S.A., Horn, K.P., Cuascut, F.X., Liu, K., He, Z., Silver, J., Flanagan, J.G., 2009. PTPsigma is a receptor for chondroitin sulfate proteoglycan, an inhibitor of neural regeneration. Science 326, 592–596.
Silver, J., Miller, J.H., 2004. Regeneration beyond the glial scar. Nat. Rev. Neurosci. 5, 146–156.
Valente, E.M., et al., 2004. Hereditary early-onset Parkinson's disease caused by mutations in PINK1. Science 304, 1158–1160.
Wauer, T., Simicek, M., Schubert, A., Komander, D., 2015. Mechanism of phospho-ubiquitin-induced PARKIN activation. Nature 524, 370–374.
Xi, Y., Dhaliwal, J.S., Ceizar, M., Vaculik, M., Kumar, K.L., Lagace, D.C., 2016. Knockout of Atg5 delays the maturation and reduces the survival of adult-generated neurons in the hippocampus. Cell Death Dis. 7, e2127.
Yi, J.J., Barnes, A.P., Hand, R., Polleux, F., Ehlers, M.D., 2010. TGF-beta signaling specifies axons during brain development. Cell 142, 144–157.
Yoshimura, T., Kawano, Y., Arimura, N., Kawabata, S., Kikuchi, A., Kaibuchi, K., 2005. GSK-3beta regulates phosphorylation of CRMP-2 and neuronal polarity. Cell 120, 137–149.
Zhang, X., Zhu, J., Yang, G.Y., Wang, Q.J., Qian, L., Chen, Y.M., Chen, F., Tao, Y., Hu, H. S., Wang, T., Luo, Z.G., 2007. Dishevelled promotes axon differentiation by regulating atypical protein kinase C. Nat. Cell Biol. 9, 743–754.